This paper is available online at www.praiseworthyprize.org
International Journal on Engineering Applications (I.R.E.A.), Vol. 10, N. 1
ISSN 2281-2881 January 2022

Design and Analysis of Renewable Energy Microgrids for Operations in Different Latitudes by Applying Fuzzy Logic Modeling

M. F. Boada[1], K. T. Prieto[1], F. Mesa[2], A. J. Aristizábal[1]

Abstract – *The modeling results presented in this work used fuzzy logic techniques to design renewable energy microgrids for operation in six cities worldwide: Dwarka, India; Shanghai, China; Milwaukee, United States; Rostock, Germany; Copenhagen, Denmark, and Kamaishi, Japan. A meticulous study on solar photovoltaic, wind potential, power demand, and population density was executed as part of this study. The results reveal that for a microgrids operative scenario comprising 50% photovoltaic solar energy and 50% wind power energy, the amount of energy that must be supplied to the six cities varies from 17,031.46 to 160,971.25 kWh/month, and the number of photovoltaic panels varies between 126 and 6,444. The number of wind turbines required varies between 3 and 11. The most significant amount of photovoltaic solar energy (546,366.41 kWh/month) generated from the microgrids was reported in Rostock, Germany. The most significant amount of generated wind power energy (277,012.15 kWh/month) was reported in Milwaukee, United States. Environmental assessments revealed that the highest amount of reduction in CO_2 emission (217.88 tonnes) was obtained from the Rostock (Germany) microgrid. The implementation of such microgrids costs ~US$ 3,903,724.*

Keywords: *Microgrids, Photovoltaic Energy, Wind Energy, Renewables, Batteries*

Nomenclature

$\tilde{A}$	Judgement matrix
AC	Alternating Current
CO_2	Carbon dioxide
C_p	Power coefficient
DC	Direct Current
E_{batt}	Battery energy
E_{load}	Energy delivered to the load
I	Current
I_d	Diode`s current
I_{ph}	Photovoltaic current
I_{sh}	Short circuit current
$I_{\max}$	Maximum current
k	Boltzmann constant
KKT	Karush Kuhn Tucker
LFP	Logarithmic Fuzzy Preference Programming
l,m,u	Real numbers
MPP	Maximum Power Point
$\widetilde{N_1}, \widetilde{N_j}$	Fuzzy Numbers
$u_{\widetilde{N}}$	Function
PV	Photovoltaic
P_{pvg}	Power of the photovoltaic generator
P_{wind}	Power of the wind
R	Rotor radius
R_{ad}	Solar radiation
ROI	Recover Over Investments
R_s	Series resistor
R_{sh}	Short circuit resistor
S	Rotor area
$\widetilde{S_i}, \widetilde{S_j}$	Functions
THD	Total Harmonic Distortion
T_{wind}	Toque of the wind
V_{batt}	Battery voltage
$V_{\max}$	Maximum voltage
V_{oc}	Open circuit voltage
V_{wind}	Wind velocity
V_t	Thermal voltage
λ	Priority vector
ρ	Air density

I. Introduction

In the last few years, there has been a worldwide increase in the installation of renewable energy microgrids, especially for photovoltaic and wind power generation, under different modes of operation using conventional electrical grids and diverse industrial, commercial and residential applications. Diverse research perspectives can be applied to microgrids. Some of the most frequently implemented research options are simulations seeking to assess the behavior of microgrids when connected to the power grid to improve their operational efficiency and economy [1], control strategies at different load conditions [2], economical delivery under different operating conditions [3] or stochastic and dynamic modeling to handle the generated

Available online by January 31st, 2022 https://doi.org/10.15866/irea.v10i1.20386

power and operating costs [4]-[6]. Different microgrid elements must be carefully analyzed because their selection determines the efficiency, reliability, and cost of the system, which must maintain frequency and voltage stability when operating at optimal voltage levels and reacting to load variations [7]. The configuration of a microgrid and its intermittent power generation produces additional emissions due to losses in energy storage systems [8]. When diverse power generation technologies are applied, including renewable and conventional ones, microgrids exhibit greater flexibility when delivering the thermal and electrical capacities based on users' demands [9]. The combined use of solar photovoltaic and wind power technologies [10], such as in cluster architectures [11] and smart grid elements in microgrids [12], is one of the most outstanding applications and innovations implemented at a global level. The types of microgrids and energy management systems depend on operational modes, financial details, and the intermittent nature of renewable energy sources [13]. Different microgrid modeling techniques can be employed [14]-[18] to determine critical aspects before and during system operation, such as stability and local management conditions, frequency and voltage dynamics, power flow analysis to determine optimal performance, and assessment of power generation sources in stable and transient conditions. In general, to validate the features in extreme operations, practical models are implemented in cases where the load variation and renewable energy generation match the real-life data [19]. Also, models are applied using fuzzy techniques to ascertain photovoltaic and wind power in the microgrid [20]. Here, conversion-storage structure optimization methodologies are also used in the microgrid planning stages [21]. Due to their unused capacity that remains available, microgrids can support other microgrids with insufficient power [22]. However, an increase in the penetration of renewable sources may increase the frequency and voltage variations within the microgrid, resulting in poor power quality within the system and a high risk of operation downtime [23].

Consequently, uncertainties in the wind and photovoltaic power generation and the electrical and thermal demands of microgrids must be assessed when introducing scenarios with their corresponding probabilities [24] and incorporating customer engagement values coupled with supply, demand, and economic cost optimization [25]. In existing electrical distribution systems, operators lack real-time monitoring capabilities for grids and consumers. However, power systems are intended to supply power to users based on their continuously changing power demands [26].

Existing power systems exhibit significant electrical losses in power distribution, especially at low voltage levels. Losses in distribution systems can be reduced through proper control of the distributed generation resources [27]. In this regard, microgrids offer high control and flexibility towards each system's reliability and power quality [28]-[32]. The operation problems of power distribution companies, including distributed generation and controllable loads, have been investigated in the literature. In [33], a two-stage hierarchical framework for distribution companies' operation considering the real-time process of energy markets is presented. In [34], the previous work is extended by considering the real-time uncertainties of electricity prices and loads. The daily scheduling of distribution companies considering energy and reserve markets are discussed in [35], [36]. The economic, environmental, and technical effects of microgrids' penetration into active power distribution grids are studied in different papers. In [37], multi-criteria decision techniques are used to evaluate microgrids' impact on distribution grids.

In the end, five criteria are presented, including installation and operation costs, investment deferral, active power losses, environmental impact, and improvement in the reliability of the distribution grid. In [38], three criteria, including economic operation, active power losses, and economic benefits, are investigated to show microgrids' impacts on utilities. In [39], an optimal control algorithm for coupling micro power grids is presented, while in [40], the scheduling of power dispatch of different microgrids operating in an isolated distribution network is investigated using multi-agent systems. In [41], the scheduling of power consumption in distribution networks with coupled microgrids considering demand uncertainty is analyzed. The problem of distribution companies and distribution networks is modeled using reference frame systems [42], [43]. Although the appropriate reference frame is selected in these papers, microgrids' distribution company operation problem is not modeled simultaneously. Initially, the microgrids' optimization problem is solved, and subsequently, the problem for the distribution companies is solved. In each iteration, the data required for the optimization are exchanged between the two systems. The iterative process continues until the convergence conditions are satisfied. A study of microgrids is made in [44] with the following contributions:

- A two-level optimization model is proposed that provides a hierarchical decision-making framework in which distribution companies and microgrids optimize their respective objective functions independently and cooperatively with each other;
- The two-level nonlinear optimization model is transformed with the single-level linear optimization model using KKT conditions and dual theory;
- A retail electricity market in distribution networks is proposed, considering distribution companies and micro-grids;
- A comparison is made between two different reference frameworks considered for the retail electricity market.

A group of researchers [45] proposes a robust optimization model of microgrids considering uncertainty to consider the economy and robustness of microgrid operation. A two-stage robust optimization

model is established to find a balance between the economy and robustness of microgrid operation. Through the optimization procedure, the robust adjustment parameters for microgrid operation can be obtained. The optimized can effectively balance the economy and robustness. Finally, a study develops a statistical framework to quantify grid-connected microgrids' resilience to ensure critical loads are served during islanding scenarios. The primary metric of resilience is microgrid survivability and is expressed as the probability for a microgrid to meet critical load requirements during an islanding event. Probabilities are evaluated using a Markov chain that describes microgrid operating states each hour for a 7-day time horizon. The system-level resilience metric uses asset-level reliability data of prominent failure modes (i.e., up-time, failure to start, failure to run) [46]. This work discusses the application of fuzzy logic modeling for the design and performance evaluation of microgrids operating in different countries under 50% photovoltaic solar energy and 50% wind power scenarios.

Section II describes the mathematical models applied in this study. Section III defines the solar and wind power potentials for the selected cities and lists the microgrid equipment used. Section IV discusses the results and technical, economic, and environmental assessments. Finally, Sections V and VI present conclusions and references, respectively.

II. Materials and Methods

II.1. Fuzzy Logic Modeling

In this study, the method developed by Wang and Chin [47], "Logarithmic Fuzzy Preference Programming (LFPP)," was applied. This method was also applied in the design of renewable power microgrids in [48]. The LFPP method is similar to the "Analytic Hierarchy Process" method, but it adds triangular fuzzy qualifications of judgments according to parameters, as shown in Fig. 1 [49]. The following fuzzy numbers are defined:

$$\widetilde{N}_1 = (l_1, m_1, u_1) \tag{1}$$

$$\widetilde{N}_2 = (l_2, m_2, u_2) \tag{2}$$

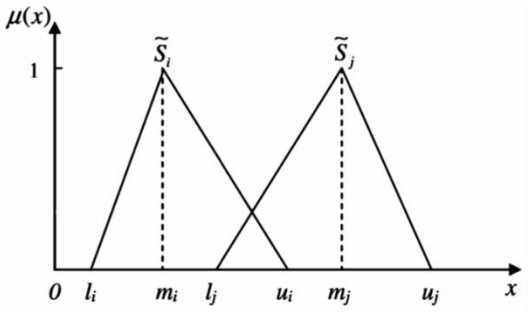

Fig. 1. Outline of functions: $\tilde{S}_i = (l_i, m_i, u_i)$ and $\tilde{S}_j = (l_j, m_j, u_j)$ (Based on data from [35])

where: *l*, *m* and *u* $\{\in \mathbb{R}\, \mathrm{I}\ > 0\}$. Mathematical operations for these fuzzy numbers will be:

Addition:

$$\begin{gathered}\widetilde{N}_1 \oplus \widetilde{N}_2 = (l_1, m_1, u_1) \oplus (l_2, m_2, u_2) = \\ = (l_1 + l_2, m_1 + m_2, u_1 + u_2)\end{gathered} \tag{3}$$

Multiplication:

$$\begin{gathered}\widetilde{N}_1 \otimes \widetilde{N}_2 = (l_1, m_1, u_1) \otimes (l_2, m_2, u_2) \cong \\ \cong (l_1 \times l_2, m_1 \times m_2, u_1 \times u_2)\end{gathered} \tag{4}$$

Division:

$$\begin{gathered}\widetilde{N}_1 \oslash \widetilde{N}_2 = (l_1, m_1, u_1) \oslash (l_2, m_2, u_2) \cong \\ \cong \left(\frac{l_1}{u_2}, \frac{m_1}{m_2}, \frac{u_1}{u_2}\right)\end{gathered} \tag{5}$$

The following steps are used in the LFPP method, according to [47]. This is the definition of the judgement matrix, $\tilde{A}$:

$$\tilde{A} = \begin{array}{c} \\ C_1 \\ C_2 \\ \vdots \\ C_n \end{array} \begin{array}{c} \begin{array}{cccc} C_1 & C_2 & \dots & C_n \end{array} \\ \begin{bmatrix} (1,1,1) & \tilde{a}_{12} & \dots & \tilde{a}_{1n} \\ \tilde{a}_{21} & (1,1,1) & \dots & \tilde{a}_{2n} \\ \vdots & \vdots & \ddots & \vdots \\ \tilde{a}_{n1} & \tilde{a}_{n2} & \dots & (1,1,1) \end{bmatrix} \end{array} \tag{6}$$

where $\tilde{a}_{ij} = \{l_{ij}, m_{ij}, u_{ij}\}\, y\ 0 < l_{ij} \le m_{ij} \le u_{ij}$. Since:

$$\ln \tilde{A}_{ij} \approx \{\ln l_{ij}, \ln m_{ij}, \ln u_{ij}\} \tag{7}$$

The following function is obtained:

$$u_{\widetilde{N}} = \begin{cases} \dfrac{x-a}{b-a}, & a \le x \le b \\ \dfrac{c-x}{c-b}, & b \le x \le c \\ 0, & \text{otherwise} \end{cases} \tag{8}$$

which can be expressed as:

$$u_{ij}\left(\ln \frac{w_i}{w_j}\right) = \begin{cases} \dfrac{\ln \frac{w_i}{w_j} - \ln l_{ij}}{\ln m_{ij} - \ln l_{ij}}, & \ln \frac{w_i}{w_j} \le \ln m_{ij} \\ \dfrac{\ln u_{ij} - \ln \frac{w_i}{w_j}}{\ln u_{ij} - \ln m_{ij}}, & \ln \frac{w_i}{w_j} \le \ln m_{ij} \end{cases} \tag{9}$$

Next, the maximization of the previous membership degree allows to calculate a priority vector:

$$\begin{gathered}\max \lambda = \min \left\{ \mu_{ij} \ln \frac{w_i}{w_j} \right\} \quad \text{with } i = 1, \dots, n-1; \\ j = i+1, \dots, n\end{gathered} \tag{10}$$

It can be expressed using the following formula:

$$\text{Maximise } 1-\lambda \quad \text{subject to} \begin{cases} \ln w_i - \ln w_j - \lambda \ln \dfrac{m_{ij}}{l_{ij}} \geq \ln l_{ij}, \\ i = 1, \ldots, n-1; j = i+1, \ldots, n \\ -\ln w_i + \ln w_j - \lambda \ln \dfrac{u_{ij}}{m_{ij}} \geq -\ln u_{ij}, \\ i = 1, \ldots, n-1; j = i+1, \ldots, n, \\ w_i =\geq 0; i = 1, \ldots, n \end{cases} \quad (11)$$

II.2. Photovoltaic Solar Cell Model

The equivalent electrical circuit of a photovoltaic solar cell is shown in Fig. 2. R_s corresponds to the electrical losses caused by the semiconductor resistive load and metallic contacts. R_p corresponds to the electrical losses caused by impurities near the p-n junction [40]. After applying Kirchoff's law, it is possible to obtain the following equation:

$$I = I_{ph} - I_d - I_{sh} \quad (12)$$

where:

$$I_d = I_0\left(e^{\frac{V+IRs}{V_t}} - 1\right) \quad (13)$$

$$I_{sh} = \frac{v + IR_s}{R_p} \quad (14)$$

After replacing this in Eq. (12), Eq. (15) is defined as follows:

$$I = I_{ph} - I_0\left(e^{\left(\frac{V+IR_s}{V_t}\right)} - 1\right) - \frac{V + IR_s}{R_p} \quad (15)$$

where I_{ph} is the current photogenerated by the solar cell, I_0 is the diode saturation current, V_t corresponds to the thermal voltage given by Eq. (16), R_s is the serial resistance and R_p corresponds to the parallel resistance:

$$V_t = \frac{mkT}{q} \quad (16)$$

where k is the Boltzman constant (1.38×10^{-23} J/K), T corresponds to the cell temperature, q is the electron's charge (1.6×10^{-19} C) and m is the diode's ideality factor ($1 < m < 2$).

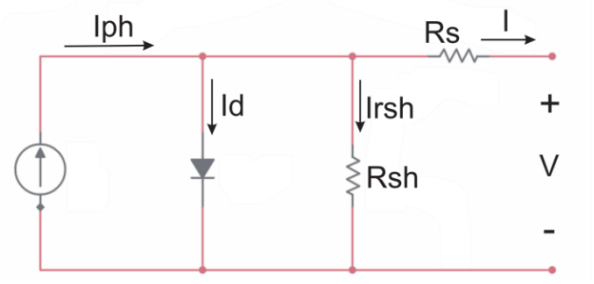

Fig. 2. Electrical circuit equivalent to a photovoltaic solar cell [34]

Therefore, the solar cell's total current can be expressed as follows:

$$I = I_{ph} - I_0\left(e^{\left(\frac{q(V+IR_s)}{mkT}\right)} - 1\right) - \frac{V + IRs}{R_p} \quad (17)$$

The following equation is applied to calculate the total power of the photovoltaic generator:

$$P_{pvg} = \frac{E_{load}}{R_{ad} \times 30 \text{ days/month}} \quad (18)$$

where P_{pvg} is the power of the photovoltaic generator (kW), E_{load} is the energy delivered to the load (kWh/month) and R_{ad} is the Solar radiation at the installation site (hours/day).

II.3. Wind Turbine Model

At the outset, the following formula is used to calculate the power coefficient [50]:

$$C_p = \frac{2P_{wind}}{\lambda S V_{wind}^3} \quad (19)$$

The power of the wind generator and the torque developed are determined using the following formulas [51]:

$$P_{wind} = \frac{1}{2} C_p(\lambda) \rho S V_{wind}^3 \quad (20)$$

$$T_{wind} = T_{mec} = \frac{1}{2} \frac{C_p(\lambda) \rho R S V_{wind}^2}{\lambda} \quad (21)$$

where S corresponds to the area covered by rotor blades (m^2), ρ is the air density, R is the rotor radius (m), V_{wind} is the wind speed (m/s) and λ equals the speed ratio of the tip. The synchronous machine model for the wind power generator is based on [52]:

$$\begin{bmatrix} V_d \\ V_q \end{bmatrix} = \begin{bmatrix} R_C & -\omega L_c \\ \omega L_c & R_c \end{bmatrix} \times \begin{bmatrix} i_d \\ i_q \end{bmatrix} + L_c \frac{d}{dt} \begin{bmatrix} i_d \\ i_q \end{bmatrix} + \begin{bmatrix} e_d \\ e_q \end{bmatrix} \quad (22)$$

II.4. Battery Model

The battery voltage of the microgrid is calculated as follows [53], [54]:

$$V_{batt} = E_{batt} - RI_{batt} \quad (23)$$

The internal battery power varies in the following manner [55]:

Charge ($i^* < 0$):

$$E_{batt} = E_0 - k_B \frac{C}{i_t + C} i^* - k_B \frac{C}{C - i_t} i_t + \alpha(t) \quad (24)$$

Discharge ($i^* > 0$):

$$E_{batt} = E_0 - k_B \frac{C}{C - i_t} i^* - k_B \frac{C}{C - i_t} i_t + \alpha(t) \quad (25)$$

$$\alpha(t) = \int \frac{B}{t(AI_{batt} - \alpha(t-1))} dt \quad (26)$$

II.5. Renewable Potentials and Microgrid Description

In the past few years, several countries have expressed interest in guiding their efforts towards a renewable future. Consequently, for the selection of six cities around the world where the analysis and dimensioning of the proposed microgrids would be conducted, a study was first made on the countries that the "Renewables Global Status Report 2018 - REN21" [56] deem as world powers in terms of photovoltaic and wind power generation and capacity.

Accordingly, the best countries were selected and, then the six coastal cities with the best solar and wind potential were determined for the study.

The first parameter considered was the energy capacity (total and per capita) or the generation capacity of solar photovoltaic and wind power energy by the end of 2017.

This analysis revealed that the country with the highest capacity is China, followed by the United States and Japan. Germany is the leader along with Denmark in per capita energy capacity, and it is the only country with participation in all four categories, occupying the first, third, and fourth positions, in that order [56] (Table I).

Other parameters used to select the participating countries were an annual investment, added net capacity, and solar photovoltaic and wind power energy production in 2017.

According to the list, as shown in Table II, China and the United States remain as leaders because they occupy the first and second positions in both lists, while India ranks third and fifth, respectively.

Similarly, Japan ranks fourth in solar photovoltaic capacity, and Germany ranks third in wind power capacity [56].

After reviewing and subjecting this data to a strict assessment, six countries were selected for the study, and the six coastal cities with the best solar and wind potentials of each country were selected: Dwarka, India; Shanghai, China; Milwaukee, United States; Rostock, Germany; Copenhagen, Denmark, and Kamaishi, Japan.

TABLE I
TOP COUNTRIES ACCORDING TO TOTAL OR GENERATION CAPACITY BY THE END OF 2017 (WIND POWER AND SOLAR PHOTOVOLTAIC POWER)

Rank	Solar PV capacity	Solar PV capacity per capita	Wind power capacity	Wind power capacity per capita
1	China	Germany	China	Denmark
2	U. S.	Japan	U. S.	Ireland
3	Japan	Belgium	Germany	Sweden
4	Germany	Italy	India	Germany
5	Italy	Australia	Spain	Portugal

TABLE II
TOP COUNTRIES ACCORDING TO ANNUAL INVESTMENT, NET CAPACITY ADDITIONS AND PRODUCTION IN 2017 (WIND POWER AND SOLAR PHOTOVOLTAIC POWER)

Position	Solar PV capacity	Wind power capacity
1	China	China
2	U. S.	U. S.
3	India	Germany
4	Japan	UK

Fig. 3 shows the monthly multiannual average of solar radiation and wind speed for an altitude of 50 m, from 1981 to 2017 for the six selected cities based on the NASA meteorological database [57]. Dwarka in India is the city with the highest solar potential. Its maximum radiation values, between March and June, exceeded 6 kWh/m^2/day. In April, a maximum radiation value of 6.92 kWh/m^2/day was recorded. Additionally, based on data analysis, it was also observed that in the 36 years of recorded data, December reports average radiation of <4.4 kWh/m^2/day. There is a total monthly multiannual average of 5.49 kWh/m^2/day. Similarly, Copenhagen, Denmark, is the city with the lowest photovoltaic potential.

From 1981 to 2017, its monthly multiannual average was 2.9 kWh/m^2/day. The lowest value recorded was in December, with 0.47 kWh/m^2/day. The best wind speed profiles corresponded to an altitude of 50 m throughout the year in Rostock, Germany, during the 36-year data assessed. This city reports an average wind speed of 7.66 m/s during the entire year. In January, a maximum wind speed of 9 m/s is reached and a minimum of 6.63 m/s in July. Kamaishi, Japan, reports the lowest wind potential with an annual average of 5.75 m/s. Here, the highest wind speeds were measured in January, February, and March between 1981 and 2017. Finally, Dwarka is the only city with a particular wind speed behavior. While the other five cities show a drop in value between April and September, in Dwarka, it increases to 8.7 m/s in July.

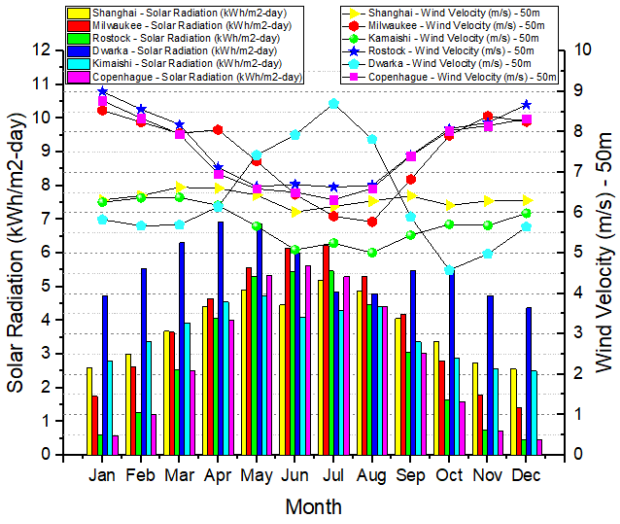

Fig. 3. Monthly multiannual average of solar radiation and wind speed for an altitude of 50 m, from 1981 to 2017 for the six selected cities [43]

In Fig. 4, the per capita electricity consumption for the six selected countries is shown, from 2000 to 2017. The United States exhibits the highest per capita energy demand, registering an average of 12,323.89 kWh/inhabitant during 2000–2017. Japan is in second place in electricity consumption, with an average of 7,373 kWh/inhabitant. Meanwhile, Denmark and Germany report a similar per capita electricity consumption. Denmark's average consumption is 6,071.16 kWh/inhabitant, and Germany has an average consumption of 6,433.16 kWh/inhabitant. China had a constant per capita electricity consumption from 2000 to 2004. In the subsequent years, accelerated growth in energy demand is observed, reaching 4,292 kWh/inhabitant in 2017. Finally, India has the lowest electricity demand. In the period analyzed, it reported an average of 514.35 kWh/inhabitant. In Table III, the population density of each country and city is shown, and the number of inhabitants per household. Shanghai, China, has the highest number of inhabitants, with 27,731,964 people and three inhabitants per household. In contrast, Milwaukee, United States, and Copenhagen, Denmark, have similar population densities, with 605,820 and 605,366 inhabitants, respectively. The same situation is also applicable to Dwarka, India, and Kamaishi, Japan, with 35,800 and 34,945 inhabitants, respectively, the two least populated cities. Dwarka is the only city with five inhabitants per household.

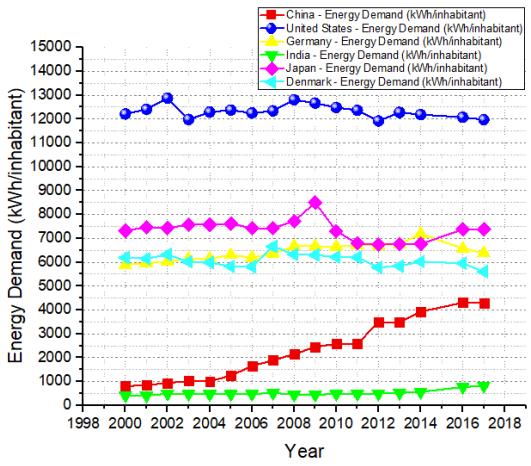

Fig. 4. Electricity demand per capita for the six selected countries [58]

TABLE III
POPULATION AND INHABITANTS PER HOUSEHOLD, 2017
(BASED ON DATA FROM [59]-[71])

Country/City	Population (Inh.)	Inhabitants/household
CHINA Shanghai	1,433,784,000 27,731,964	3
UNITED STATES Milwaukee	329,065,000 605,829	3
GERMANY Rostock	83,517,000 208,261	3
INDIA Dwarka	1,366,418,000 35,800	5
JAPAN Kamaishi	126,860,000 34,945	3
DENMARK Copenhagen	5,772,000 605,366	3

Fig. 5 shows the microgrid scheme designed for each city. In each city, the microgrid will be designed to deliver power to groups of 50 housing units. The photovoltaic, and wind power generators will be responsible for supplying the potential load demand and a battery storage system will be used for the storage of surplus energy.

For optimal operation, this battery set will be controlled by a set of islanded inverters. If the renewable sources do not have sufficient power generation capacity to supply the load, the electrical grid will operate as support. Table IV lists the technical specifications of the photovoltaic solar panel selected for the microgrids. The photovoltaic solar panel was selected based on its high efficiency and good global availability. Its technology employs monocrystalline silicon, and it costs US$ 0.23/W (24-199 pieces). The selected wind turbine has a power of 120 kW; its AC frequency and rotor diameters are 60 Hz and 19.4 m, respectively, and it has three blades [73]. The specifications of the DC/AC inverter selected for the photovoltaic generator are shown in Table V.

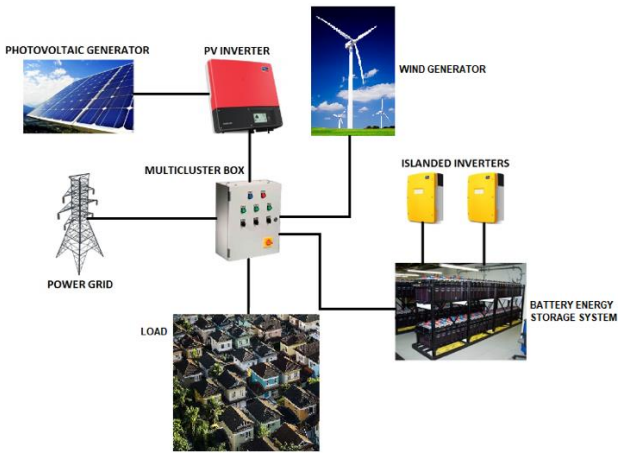

Fig. 5. Microgrid functional structure to be designed

TABLE IV
ELECTRICAL PARAMETERS FOR THE SELECTED PHOTOVOLTAIC PANEL (BASED ON DATA FROM [72])

Item	Electrical specifications
Model number	JX500M
Power	500 W
VOC	58.95 V
ISC	10.87 A
I max	10.28 A
V max	48.63 V
Efficiency	19.51%

TABLE V
ELECTRICAL PARAMETERS OF THE SELECTED DC/AC INVERTER
(BASED ON DATA FROM [74])

Item	Electrical specifications
Rated DC power	61240 W
MPP voltage range	598–800 V
Rated AC power	60000 W
AC Frequency	50 Hz/60 Hz
Efficiency	98%
THD	<3%
Max. Output current	82.5 A

III. Results and Discussion

III.1. Technical Results

For the microgrids, an operative scenario is defined, in which 50% of the energy demand of the load was supplied by solar energy and the remaining 50% was supplied by wind power. Table VI lists the number of inhabitants for each household and per set of 50 households established as microgrid load. Based on the modeling techniques listed in Section II and data presented in Section II, the following pages' results were obtained. According to the per capita energy demand during 2000–2017 shown in Fig. 4, Table VII lists the energy demand that each microgrid must cover.

TABLE VI
TOTAL NUMBER OF INHABITANTS FOR THE MICROGRID DESIGN

Country	Inhabitants per household	Inhabitants per set
Shanghai (China)	3	150
Milwaukee (United States)	3	150
Rostock (Germany)	3	150
Dwarka (India)	5	250
Kamaishi (Japan)	3	150
Copenhagen (Denmark)	3	150

TABLE VII
ENERGY TO BE SUPPLIED TO EACH SET OF 50 HOUSEHOLDS IN EACH CITY PER MONTH FOR THE PROPOSED INHABITANTS

Country	Maximum electricity consumption per capita between 2000 and 2018 (kWh/inh.)	Power to be supplied (kWh/month)
Shanghai (China)	4310.03	53875.38
Milwaukee (United States)	12877.7	160971.25
Rostock (Germany)	7191.65	89895.63
Dwarka (India)	817.51	17031.46
Kamaishi (Japan)	8498.67	106233.38
Copenhagen (Denmark)	6658.6	83232.50

To meet these energy demands for each city, the microgrid equipment sizing yielded the results of Table VIII. As both Rostock and Copenhagen have relatively low solar energy potential (as shown in Fig. 3), they need the most significant amount of photovoltaic power generation to cover 50% of their demand: 3,222 kW (6,444 panels of 500 W each) and 2856.3 kW (5,713 panels of 500 W each), respectively. To cover the remaining 50% of the demand, Rostock and Copenhagen require four 120-kW wind power turbines. In contrast, Dwarka and Shanghai have the best solar energy potential all year round. Therefore, they need the smallest photovoltaic power generators for their microgrids: 62.86 kW and 339.44 kW, respectively. In the United States, Milwaukee has good solar and wind potential. However, based on the significant energy demand per capita, this city needs eleven wind turbines and 3,657 photovoltaic panels to meet 100% of its demand. In Figs. 6, the results of DC energy generated by solar panels and by wind turbines on a monthly basis are presented. From the highest to the lowest solar panel power generation, the cities are ranked as follows: Rostock with 546,366.41 kWh/month in July, Copenhagen with 480 715.29 kWh/month in June, Milwaukee with 352 550.16 kWh/month in July, Kamaishi with 101,811.07 kWh/month in May, Shanghai with 54,612.50 kWh/month in July and Dwarka with 13,406.78 kWh/month in April. Also, the cities are ranked by wind power generation as follows: Milwaukee with 277,012.15 kWh/month in January, Rostock with 118,316.84 kWh/month in January, Kamaishi with 115,908.09 kWh/month in March, Copenhagen with 109,475.72 kWh/month in January, Dwarka with 53,437.58 kWh/month in July and Shanghai with 35,474.88 kWh/month in March. The variation in the incident energy on the photovoltaic power generator and solar radiation available for each microgrid are shown in Figs. 7. The highest incident energies on photovoltaic generators are reported in Kamaishi, Dwarka, and Shanghai as there are good solar radiation levels in these cities. However, it's necessary also consider that areas occupied by solar panels influence the parameter calculations. Furthermore, Milwaukee, Rostock, and Copenhagen's monthly solar radiation behavior is similar because they report the lowest radiation during September–March. Therefore, during these periods, the incident energy of photovoltaic generators is the lowest.

Fig. 8 shows the energy generated by microgrids and the AC energy variation in the photovoltaic inverters' power for each city. The maximum annual microgrid energy was recorded in Milwaukee, with 4,851,126.36 kWh/year, while Rostock reported the maximum inverter energy with 3,023,595.81 kWh/year. Copenhagen and Kamaishi generated intermediate levels among these six cities regarding microgrid and solar inverter power generation capacity. The microgrids in Shanghai and Dwarka generated the lowest total power output from both microgrids and inverters.

TABLE VIII
TECHNICAL ANALYSIS OF THE 50% SOLAR AND THE 50% WIND POWER ENERGY SUPPLY

CITY	Peak generator power (kW)	Panel Power (W)	Number of panels	Inverter Output Power (kW)	Amount of DC / AC inverters	Amount Inverters for Batteries	Number of Batteries	Amount Multicluster Box (100 kW)	Number of turbines (120 kW)
Shanghai, China	339,44	500	679	305,49	6	18	6	4	3
Milwaukee, United States	1828,39	500	3657	1645,55	29	99	17	19	11
Rostock, Germany	3222,07	500	6444	2899,86	49	174	9	33	4
Dwarka, India	62,86	500	126	56,57	1	3	2	1	2
Kamaishi, Japan	694,34	500	1389	624,90	12	37	11	7	11
Copenhague, Denmark	2856,30	500	5713	2570,67	43	154	9	29	4

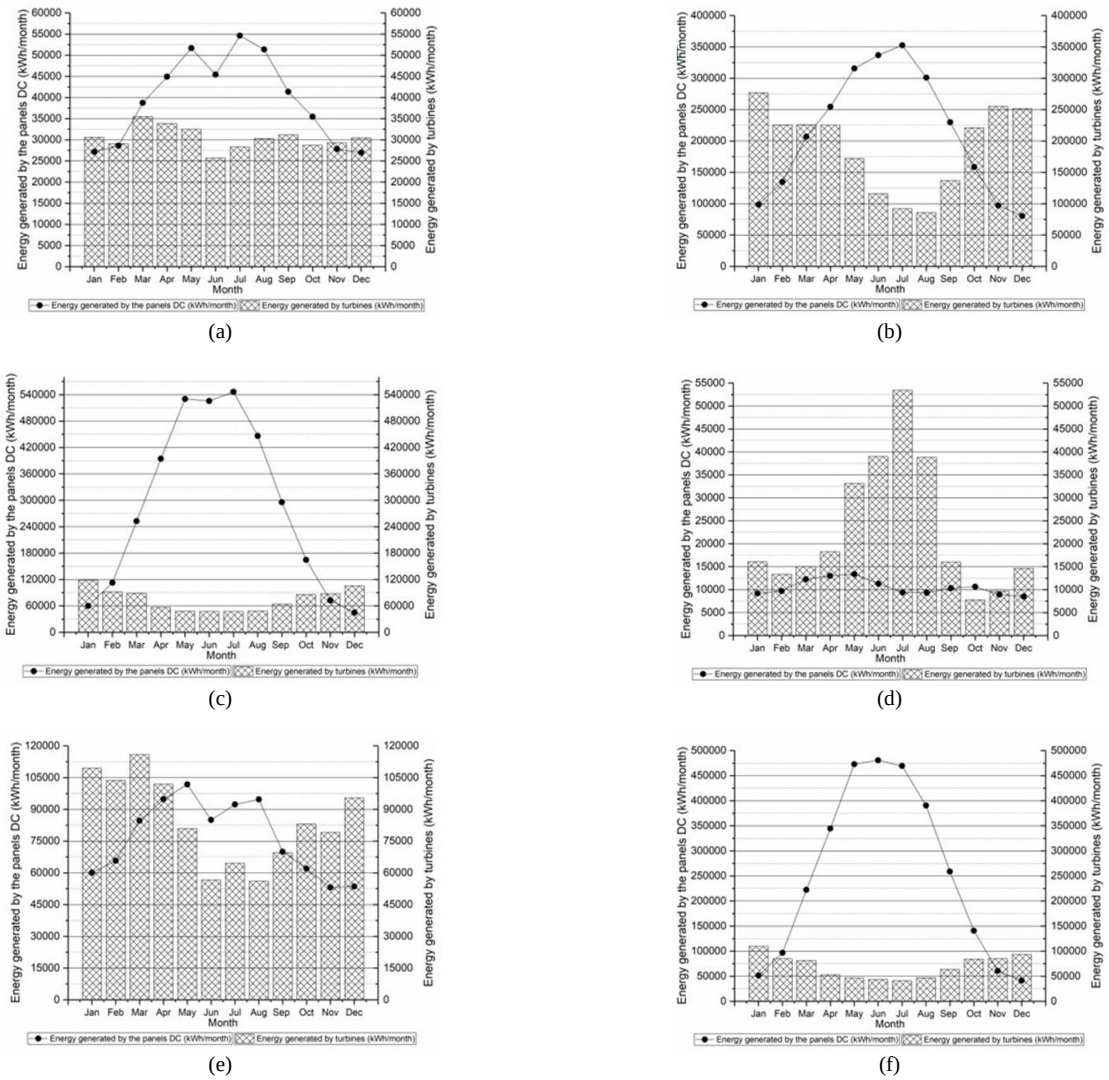

Figs. 6. Energy generated by solar panels and wind turbines: (a) Shanghai, China; (b) Milwaukee, United States; (c) Rostock, Germany; (d) Dwarka, India; (e) Kamaishi, Japan; (f) Copenhagen, Denmark

III.2. Environmental Results

The reduction in the monthly amount of CO_2 emission and the monthly amount of energy generated are shown in Figs. 9. The maximum reduction in the amount of CO_2 emission and energy produced by microgrids are:

- 30.89 tonnes and 84,177.73 kWh/month, respectively, for Shanghai (a);
- 179.06 tonnes and 487,913.15 kWh/month for Milwaukee (b);
- 217.88 tonnes and 593,666.24 kWh/month for Rostock (c);
- 23.07 tonnes and 62,869.1 kWh/month for Dwarka (d);
- 73.58 tonnes and 200,499.54 kWh/month for Kamaishi (e);
- 192.33 tonnes and 524048.57 kWh/month for Copenhagen (f).

The reduction in the amount of CO_2 emission and the amount of energy generated by microgrids per year are presented in Fig. 10. As it can be observed, the Milwaukee microgrid showed the maximum reduction in the amount of CO_2 emission with 1,780.36 tonnes/year, and this microgrid generates 4,851,126.36 kWh of energy per year. Rostock ranks second (1,654 tonnes/year) and generated over 43,000 kWh/year of energy. In terms of the amount of energy produced, the microgrids in Shanghai and Dwarka prevent the emission of the least amount of CO_2, based on their solar photovoltaic and wind power usage.

III.3. Economic Results

Fig. 11 illustrates the economic investment in US dollars for each microgrid and the return on each city's investment period. Costs were calculated considering equipment and material prices and installation and commissioning costs. The most significant economic investment is for Rostock, Germany, microgrid, with a total of US$ 3,846,700, and its return on investment, calculated based on current energy prices in this city, is 11.9 years.

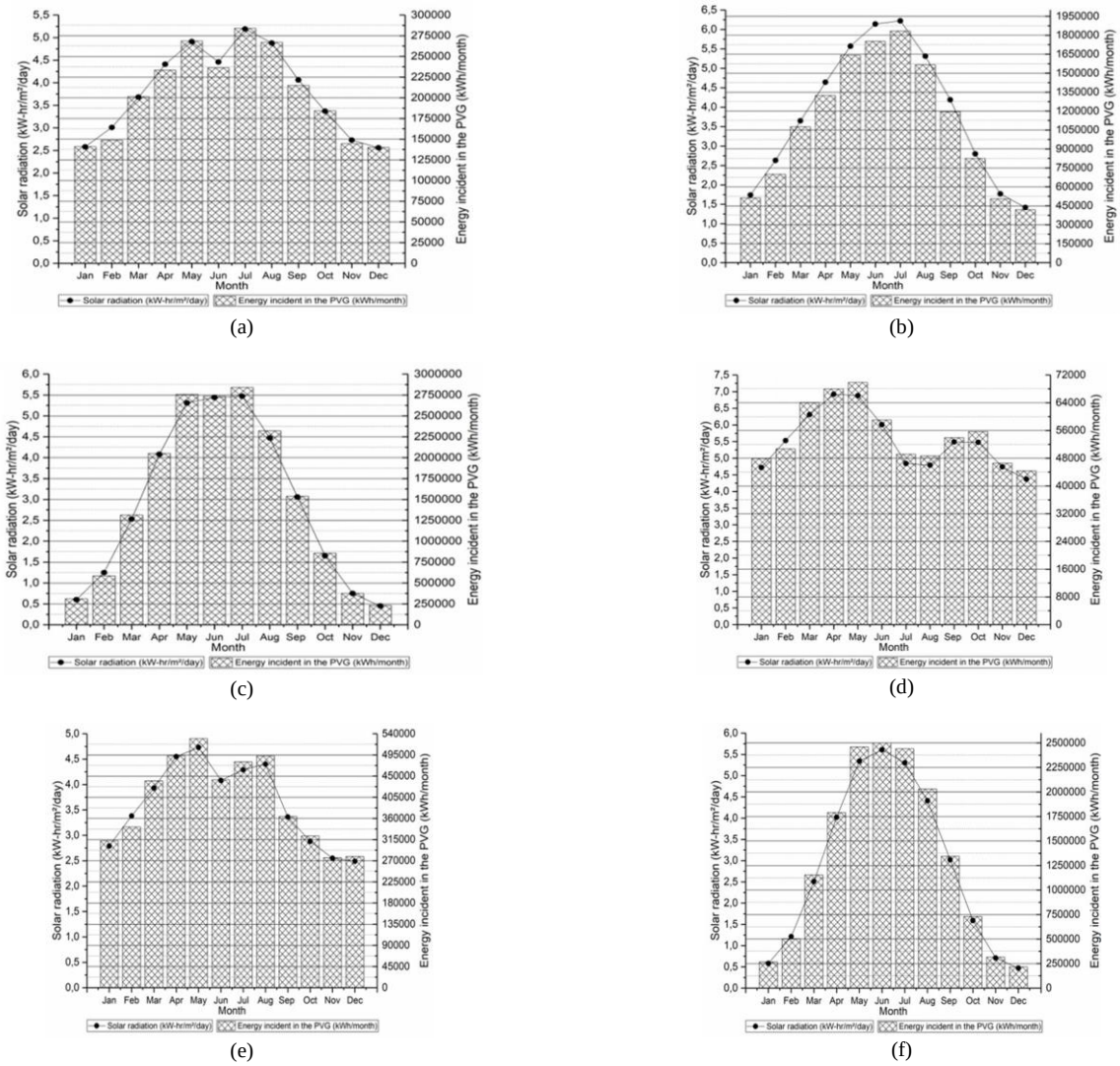

Figs. 7. Energy incident in the PVG and solar radiation for each microgrid: a) Shanghai, China; b) Milwaukee, United States; c) Rostock, Germany; d) Dwarka, India; (e) Kamaishi, Japan; f) Copenhagen, Denmark

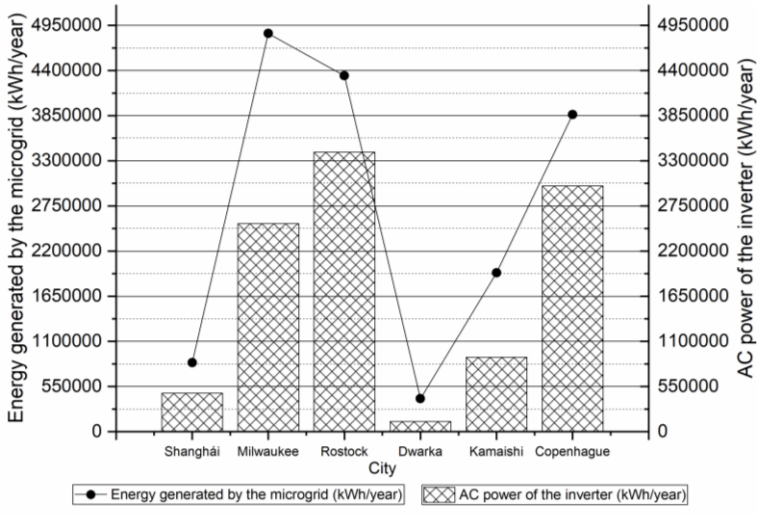

Fig. 8. Variation in the microgrid-generated energy
and the AC energy of photovoltaic inverters

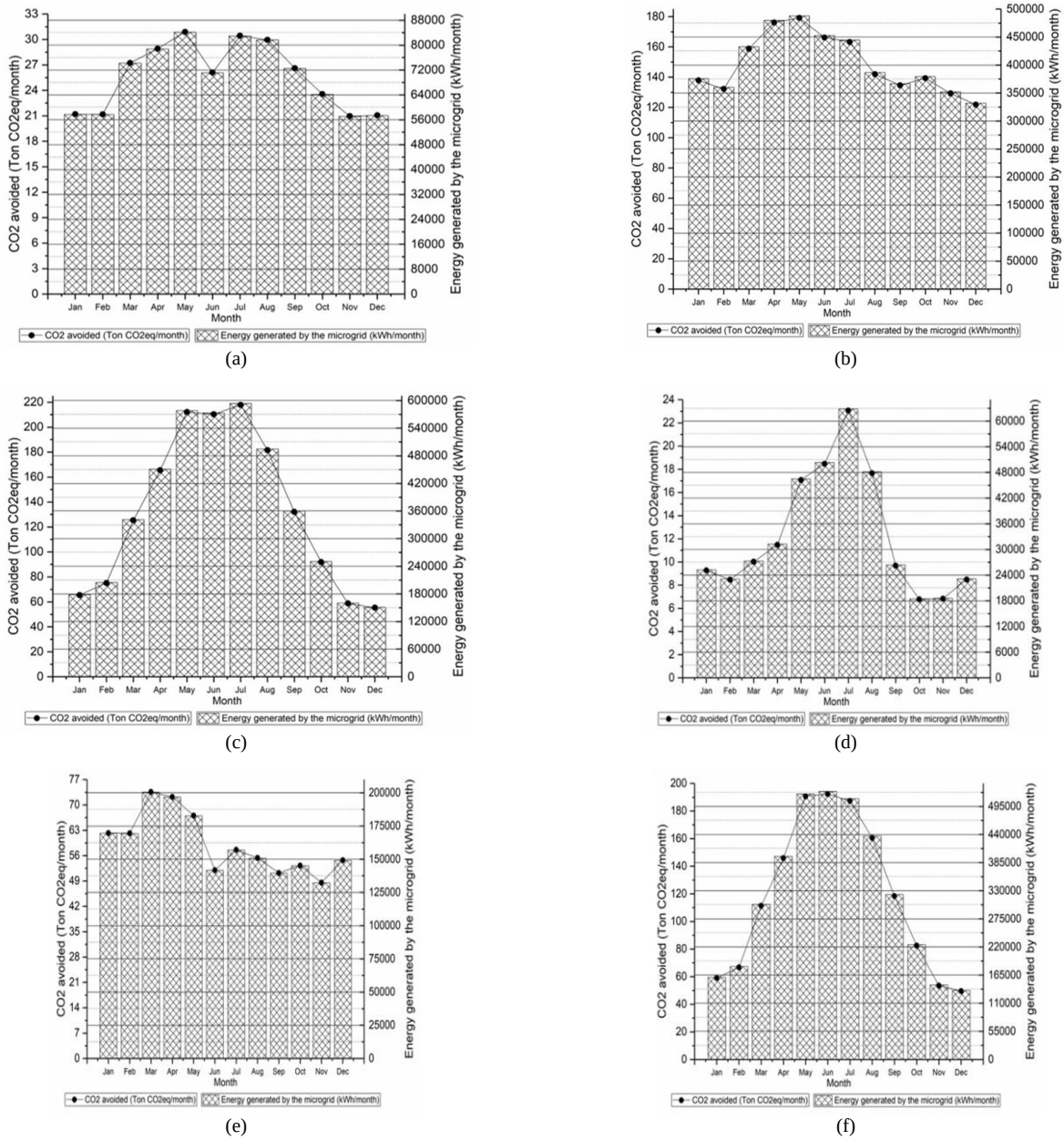

Figs. 9. Reduction in the amount of CO_2 emission and energy generated by microgrids: (a) Shanghai, China; (b) Milwaukee, United States; (c) Rostock, Germany; (d) Dwarka, India; (e) Kamaishi, Japan; (f) Copenhagen, Denmark

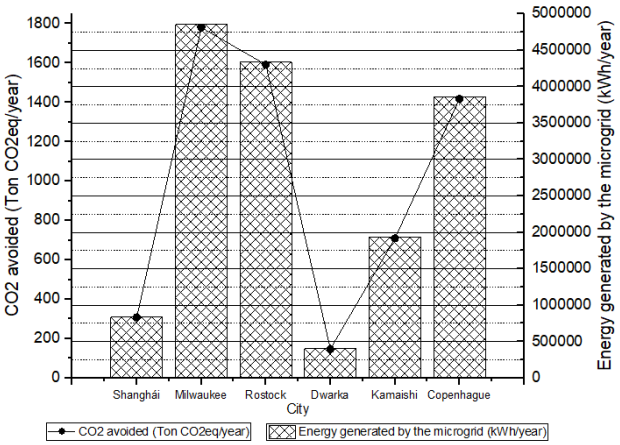

Fig. 10. Annual variation in the reduction in the amount of CO_2 emission and energy generated by each microgrid

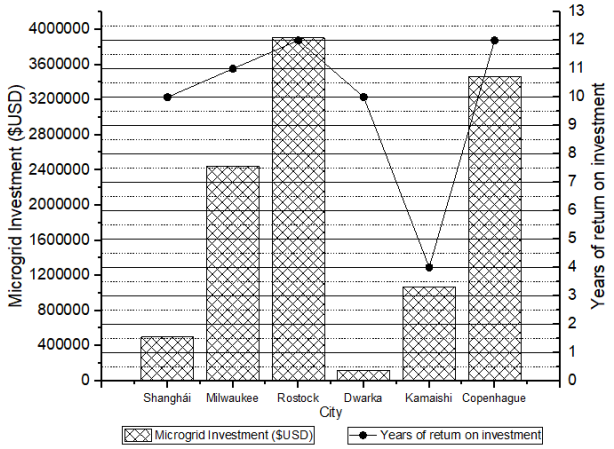

Fig. 11. Economic investment for microgrids and variations of payback periods in years

Copenhagen requires an economic investment of US$ 3,564,300 to install the proposed microgrid, and its return on investment period would be 12.1 years. Milwaukee requires an investment of US$ 2,410,000, which could be recovered after the first 11 years of microgrid operations. Shanghai and Dwarka are the cities that require minor economic investments for microgrids and their return on investment periods are under 1.6 years.

IV. Conclusion

This paper includes a meticulous study on assessing the solar and wind power potential of the six different cities selected, along with the per capita energy demand and their population densities. Fuzzy logic modeling techniques have proven to be suitable for microgrid design and their technical, environmental, and economic analyses. Also, these techniques can be applied to cities located in different latitudes. The solar and wind potential of a particular site will largely define the microgrid generation capacity as they directly affect the number of solar panels and wind turbines needed for these applications. However, the load energy demands must also be considered to impact the economic investment required and its return on investment period.

Although the financial investments for some of these microgrids exceed US$ 3.8 million, all microgrids for all the cities assessed are viable as the most extended ROI term corresponds to less than 12.1 years for the most critical case. This accounts for the great benefits that renewable sources currently provide due to their constant price drop. As future improvements, authors propose to add biomass to include within the design of the microgrids.

This will make it possible to take advantage of the enormous biomass resources of the countries analyzed. It would also allow increasing the size of the fuzzy logic model, and it would be possible to have an additional source of energy that improves the reliability of the microgrids.

Acknowledgements

The Universidad de Bogota Jorge Tadeo Lozano and Universidad del Rosario, supported this work.

References

[1] Y. Du et al., A cooperative game approach for coordinating multi-microgrid operation within distribution systems, *Applied Energy*, vol. 222, pp. 383–395, Jul. 2018. doi: 10.1016/j.apenergy.2018.03.086

[2] J. Hu, Y. Xu, K. W. Cheng, and J. M. Guerrero, A model predictive control strategy of PV-Battery microgrid under variable power generations and load conditions, *Applied Energy*, vol. 221, pp. 195–203, Jul. 2018. doi: 10.1016/j.apenergy.2018.03.085

[3] V. Bhattacharjee and I. Khan, A non-linear convex cost model for economic dispatch in microgrids, *Applied Energy*, vol. 222, pp. 637–648, Jul. 2018. doi: 10.1016/j.apenergy.2018.04.001

[4] I. Zafeiratou, I. Prodan, L. Lefèvre, and L. Piétrac, Dynamical modelling of a DC microgrid using a port-Hamiltonian formalism, *IFAC-PapersOnLine*, vol. 51, no. 2, pp. 469–474, Jan. 2018. doi: 10.1016/j.ifacol.2018.03.079

[5] Y. Zhang, F. Meng, R. Wang, W. Zhu, and X.-J. Zeng, A stochastic MPC based approach to integrated energy management in microgrids, *Sustainable Cities and Society*, vol. 41, pp. 349–362, Aug. 2018. doi: 10.1016/j.scs.2018.05.044

[6] N. J. Williams, P. Jaramillo, and J. Taneja, An investment risk assessment of microgrid utilities for rural electrification using the stochastic techno-economic microgrid model: A case study in Rwanda, *Energy for Sustainable Development*, vol. 42, pp. 87–96, Feb. 2018. doi: 10.1016/j.esd.2017.09.012

[7] R. C. Matthews, W. W. Weaver, R. D. Robinett, and D. G. Wilson, Hamiltonian methods of modeling and control of AC microgrids with spinning machines and inverters, *International Journal of Electrical Power & Energy Systems*, vol. 98, pp. 315–322, Jun. 2018. doi: 10.1016/j.ijepes.2017.11.041

[8] Q. Kong, M. Fowler, E. Entchev, and H. Ribberink, Impact assessment of microgrid implementation considering complementary building operation: An Ontario, Canada case, *Energy Conversion and Management*, vol. 168, pp. 564–575, Jul. 2018. doi: 10.1016/j.enconman.2018.05.033

[9] B. Aluisio, M. Dicorato, G. Forte, G. Litrico, and M. Trovato, Integration of heat production and thermal comfort models in microgrid operation planning, *Sustainable Energy, Grids and Networks*, vol. 16, pp. 37–54, Dec. 2018. doi: 10.1016/j.segan.2018.05.004

[10] B. Domenech, M. Ranaboldo, L. Ferrer-Martí, R. Pastor, and D. Flynn, Local and regional microgrid models to optimise the design of isolated electrification projects, *Renewable Energy*, vol. 119, pp. 795–808, Apr. 2018. doi: 10.1016/j.renene.2017.10.060

[11] E. Bullich-Massagué, F. Díaz-González, M. Aragüés-Peñalba, F. Girbau-Llistuella, P. Olivella-Rosell, and A. Sumper, Microgrid clustering architectures, *Applied Energy*, vol. 212, pp. 340–361, Feb. 2018. doi: 10.1016/j.apenergy.2017.12.048

[12] F. Guzzi, D. Neves, and C. A. Silva, Integration of smart grid mechanisms on microgrids energy modelling, *Energy*, vol. 129, pp. 321–330, Jun. 2017. doi: 10.1016/j.energy.2017.04.084

[13] M. F. Zia, E. Elbouchikhi, and M. Benbouzid, Microgrids energy management systems: A critical review on methods, solutions, and prospects, *Applied Energy*, vol. 222, pp. 1033–1055, Jul. 2018. doi: 10.1016/j.apenergy.2018.04.103

[14] A. Alzahrani, M. Ferdowsi, P. Shamsi, and C. H. Dagli, Modeling and Simulation of Microgrid, *Procedia Computer Science*, vol.

114, pp. 392–400, Jan. 2017.
doi: 10.1016/j.procs.2017.09.053

[15] B. Hammer, K. Gong, and U. Konigorski, Modeling and control of inverter-based microgrids, *IFAC-PapersOnLine*, vol. 51, no. 2, pp. 19–24, Jan. 2018.
doi: 10.1016/j.ifacol.2018.03.004

[16] J. Kitson et al., Modelling of an expandable, reconfigurable, renewable DC microgrid for off-grid communities, *Energy*, vol. 160, pp. 142–153, Oct. 2018.
doi: 10.1016/j.energy.2018.06.219

[17] L. Zhu and D. J. Hill, Modeling and Stability of Microgrids with Smart Loads, *IFAC-PapersOnLine*, vol. 50, no. 1, pp. 10021–10026, Jul. 2017.
doi: 10.1016/j.ifacol.2017.08.2037

[18] M. Ilić, R. Jaddivada, and X. Miao, Modeling and analysis methods for assessing stability of microgrids, *IFAC-PapersOnLine*, vol. 50, no. 1, pp. 5448–5455, Jul. 2017.
doi: 10.1016/j.ifacol.2017.08.1081

[19] S. Boudoudouh and M. Maâroufi, Multi agent system solution to microgrid implementation, *Sustainable Cities and Society*, vol. 39, pp. 252–261, May 2018.
doi: 10.1016/j.scs.2018.02.020

[20] Y.-Y. Hong, W.-C. Chang, Y.-R. Chang, Y.-D. Lee, and D.-C. Ouyang, Optimal sizing of renewable energy generations in a community microgrid using Markov model, *Energy*, vol. 135, pp. 68–74, Sep. 2017.
doi: 10.1016/j.energy.2017.06.098

[21] J. Wasilewski, Optimisation of multicarrier microgrid layout using selected metaheuristics, *International Journal of Electrical Power & Energy Systems*, vol. 99, pp. 246–260, Jul. 2018.
doi: 10.1016/j.ijepes.2018.01.022

[22] A. Albaker, A. Majzoobi, G. Zhao, J. Zhang, and A. Khodaei, Privacy-preserving optimal scheduling of integrated microgrids, *Electric Power Systems Research*, vol. 163, pp. 164–173, Oct. 2018.
doi: 10.1016/j.epsr.2018.06.007

[23] M. C. Magro, M. Giannettoni, P. Pinceti, and M. Vanti, Real time simulator for microgrids, *Electric Power Systems Research*, vol. 160, pp. 381–396, Jul. 2018.
doi: 10.1016/j.epsr.2018.03.018

[24] M. H. Shams, M. Shahabi, and M. E. Khodayar, Stochastic day-ahead scheduling of multiple energy Carrier microgrids with demand response, *Energy*, vol. 155, pp. 326–338, Jul. 2018.
doi: 10.1016/j.energy.2018.04.190

[25] G. Prinsloo, R. Dobson, and A. Mammoli, Synthesis of an intelligent rural village microgrid control strategy based on smartgrid multi-agent modelling and transactive energy management principles, *Energy*, vol. 147, pp. 263–278, Mar. 2018.
doi: 10.1016/j.energy.2018.01.056

[26] H. Abdi, S. D. Beigvand, and M. L. Scala, A review of optimal power flow studies applied to smart grids and microgrids, *Renewable and Sustainable Energy Reviews*, vol. 71, pp. 742–766, May 2017, doi: 10.1016/j.rser.2016.12.102.

[27] A. M. Bouzid, J. M. Guerrero, A. Cheriti, M. Bouhamida, P. Sicard, and M. Benghanem, A survey on control of electric power distributed generation systems for microgrid applications, *Renewable and Sustainable Energy Reviews*, vol. 44, pp. 751–766, Apr. 2015.
doi: 10.1016/j.rser.2015.01.016

[28] M. Mahmoodi, P. Shamsi, and B. Fahimi, Economic Dispatch of a Hybrid Microgrid With Distributed Energy Storage, *IEEE Transactions on Smart Grid*, vol. 6, no. 6, pp. 2607–2614, Nov. 2015.
doi: 10.1109/TSG.2014.2384031

[29] A. H. Fathima and K. Palanisamy, Optimization in microgrids with hybrid energy systems – A review, *Renewable and Sustainable Energy Reviews*, vol. 45, pp. 431–446, May 2015.
doi: 10.1016/j.rser.2015.01.059

[30] N. W. A. Lidula and A. D. Rajapakse, Microgrids research: A review of experimental microgrids and test systems, *Renewable and Sustainable Energy Reviews*, vol. 15, no. 1, pp. 186–202, Jan. 2011.
doi: 10.1016/j.rser.2010.09.041

[31] J. Hare, X. Shi, S. Gupta, and A. Bazzi, Fault diagnostics in smart micro-grids: A survey, *Renewable and Sustainable Energy Reviews*, vol. 60, pp. 1114–1124, Jul. 2016.
doi: 10.1016/j.rser.2016.01.122

[32] L. Zhang, N. Gari, and L. V. Hmurcik, Energy management in a microgrid with distributed energy resources, *Energy Conversion and Management*, vol. 78, pp. 297–305, Feb. 2014.
doi: 10.1016/j.enconman.2013.10.065

[33] I. L. R. Gomes, R. Melicio, and V. M. F. Mendes, A novel microgrid support management system based on stochastic mixed-integer linear programming, *Energy*, vol. 223, p. 120030, May 2021.
doi: 10.1016/j.energy.2021.120030

[34] H. Qian, Q. Xu, Y. Xia, P. Du, and J. Zhao, Control and synchronization of a fixed-frequency control method in microgrid based on global positioning system, *Energy Reports*, vol. 6, pp. 978–984, Dec. 2020.
doi: 10.1016/j.egyr.2020.11.089

[35] M. Adly and K. Strunz, DC microgrid small-signal stability and control: Sufficient stability criterion and stabilizer design, *Sustainable Energy, Grids and Networks*, vol. 26, p. 100435, Jun. 2021.
doi: 10.1016/j.segan.2021.100435

[36] J. Wang, A. Pratt, K. Prabakar, B. Miller, and M. Symko-Davies, Development of an integrated platform for hardware-in-the-loop evaluation of microgrids prior to site commissioning, *Applied Energy*, vol. 290, p. 116755, May 2021.
doi: 10.1016/j.apenergy.2021.116755

[37] Y. Li, J. Yang, H. Wang, J. Cui, Y. Ma, and S. Huang, Dynamic equivalent modeling for microgrid based on GRU, *Energy Reports*, vol. 6, pp. 1291–1297, Dec. 2020.
doi: 10.1016/j.egyr.2020.11.041

[38] H. Xu, Z. Meng, and Y. Wang, Economic dispatching of microgrid considering renewable energy uncertainty and demand side response, *Energy Reports*, vol. 6, pp. 196–204, Dec. 2020.
doi: 10.1016/j.egyr.2020.11.261

[39] M. A. Aftab, S. M. S. Hussain, A. Latif, D. C. Das, and T. S. Ustun, IEC 61850 communication based dual stage load frequency controller for isolated hybrid microgrid, *International Journal of Electrical Power & Energy Systems*, vol. 130, p. 106909, Sep. 2021.
doi: 10.1016/j.ijepes.2021.106909

[40] K. N. Dharmalingam et al., Investigation on microgrid control for grid tied PV battery system incorporating sustainable manufacturing technology, *Materials Today: Proceedings*, Oct. 2020.
doi: 10.1016/j.matpr.2020.09.273

[41] S. Lenhart and K. Araújo, Microgrid decision-making by public power utilities in the United States: A critical assessment of adoption and technological profiles, *Renewable and Sustainable Energy Reviews*, vol. 139, no. C, 2021, Accessed: Mar. 10, 2021. [Online]. Available: https://ideas.repec.org/a/eee/rensus/v139y2021ics136403212030976x.html

[42] A. Ouammi, Peak load reduction with a solar PV-based smart microgrid and vehicle-to-building (V2B) concept, *Sustainable Energy Technologies and Assessments*, vol. 44, p. 101027, Apr. 2021.
doi: 10.1016/j.seta.2021.101027

[43] M. Restrepo, C. A. Cañizares, J. W. Simpson-Porco, P. Su, and J. Taruc, Optimization- and Rule-based Energy Management Systems at the Canadian Renewable Energy Laboratory microgrid facility, *Applied Energy*, vol. 290, p. 116760, May 2021.
doi: 10.1016/j.apenergy.2021.116760

[44] A. Chandra, G. K. Singh, and V. Pant, Protection of AC microgrid integrated with renewable energy sources – A research review and future trends, *Electric Power Systems Research*, vol. 193, p. 107036, Apr. 2021.
doi: 10.1016/j.epsr.2021.107036

[45] J. Yang and C. Su, Robust optimization of microgrid based on renewable distributed power generation and load demand uncertainty, *Energy*, vol. 223, p. 120043, May 2021.
doi: 10.1016/j.energy.2021.120043

[46] J. Nelson, N. G. Johnson, K. Fahy, and T. A. Hansen, Statistical

development of microgrid resilience during islanding operations, *Applied Energy*, vol. 279, p. 115724, Dec. 2020. doi: 10.1016/j.apenergy.2020.115724
[47] Y.-M. Wang and K.-S. Chin, Fuzzy analytic hierarchy process: A logarithmic fuzzy preference programming methodology, *International Journal of Approximate Reasoning*, vol. 52, no. 4, pp. 541–553, Jun. 2011. doi: 10.1016/j.ijar.2010.12.004
[48] A. J. Aristizábal, D. H. Ospina, M. Castañeda, S. Zapata, and E. Banguero, Fuzzy logic energy management for a microgrid with storage battery, *International Journal of Ambient Energy*, vol. 41, no. 10, pp. 1183–1191, Aug. 2020. doi: 10.1080/01430750.2018.1507931
[49] G. van de Kaa, J. Rezaei, L. Kamp, and A. de Winter, Photovoltaic technology selection: A fuzzy MCDM approach, *Renewable and Sustainable Energy Reviews*, vol. 32, pp. 662–670, Apr. 2014. doi: 10.1016/j.rser.2014.01.044
[50] A. Tomilson, J. Quaicoe, R. Gosine, M. Hinchey, and N. Bose, Modelling an autonomous wind-diesel system using SIMULINK, in *CCECE '97. Canadian Conference on Electrical and Computer Engineering. Engineering Innovation: Voyage of Discovery. Conference Proceedings*, May 1997, vol. 1, pp. 35–38 vol.1. doi: 10.1109/CCECE.1997.614783
[51] B. Belvedere, M. Bianchi, A. Borghetti, C. A. Nucci, M. Paolone, and A. Peretto, A Microcontroller-Based Power Management System for Standalone Microgrids With Hybrid Power Supply, *IEEE Transactions on Sustainable Energy*, vol. 3, no. 3, pp. 422–431, Jul. 2012. doi: 10.1109/TSTE.2012.2188654
[52] D. Rekioua, Wind Energy Conversion and Power Electronics Modeling, in *Wind Power Electric Systems: Modeling, Simulation and Control*, D. Rekioua, Ed. London: Springer, 2014, pp. 51–76.
[53] M. Bechouat, Y. Soufi, M. Sedraoui, and S. Kahla, Energy storage based on maximum power point tracking in photovoltaic systems: A comparison between GAs and PSO approaches, *International Journal of Hydrogen Energy*, vol. 40, no. 39, pp. 13737–13748, Oct. 2015. doi: 10.1016/j.ijhydene.2015.05.008
[54] H. Fathabadi, Fuel cell/back-up battery hybrid energy conversion systems: Dynamic modeling and harmonic considerations, *Energy Conversion and Management*, vol. 103, pp. 573–584, Oct. 2015. doi: 10.1016/j.enconman.2015.07.010
[55] A. Rezvani, A. Khalili, A. Mazareie, and M. Gandomkar, Modeling, control, and simulation of grid connected intelligent hybrid battery/photovoltaic system using new hybrid fuzzy-neural method, *ISA Transactions*, vol. 63, pp. 448–460, Jul. 2016. doi: 10.1016/j.isatra.2016.02.013
[56] Ren21 2018. https://www.ren21.net/gsr-2018/
[57] NASA. https://power.larc.nasa.gov/data-access-viewer/
[58] Download the World Factbook — Central Intelligence Agency. (accessed Sep. 03, 2020). https://www.cia.gov/library/publications/download
[59] United Nations Population Division | Department of Economic and Social Affairs. (accessed Sep. 03, 2020). https://www.un.org/en/development/desa/population/index.asp
[60] Shangai Population. (accessed Sep. 03, 2020). http://poblacion.population.city/china/shanghai/
[61] Chinese society in data - Present *Stories from China*, Feb. 19, 2017. (accessed Sep. 03, 2020). https://www.historiasdechina.com/2017/02/19/la-sociedad-china-en-datos/
[62] Milwaukee · Population. (accessed Sep. 03, 2020). http://poblacion.population.city/estados-unidos/milwaukee/
[63] U.S. Census Bureau QuickFacts: United States. (accessed Sep. 03, 2020). https://www.census.gov/quickfacts/fact/table/US/PST045219
[64] Rostock | UBC.net. (accessed Sep. 03, 2020). https://www.ubc.net/cities/rostock
[65] Reach the german consumer-Santandertrade.com.(accessed Sep. 03, 2020). https://santandertrade.com/es/portal/analizar-mercados/alemania/llegar-al-consumidor
[66] Dwarka, *Mapcarta*. (accessed Sep. 03, 2020). https://mapcarta.com/es/Dwarka
[67] Reach the indian consumer - Santandertrade.com. (accessed Sep. 03, 2020). https://santandertrade.com/es/portal/analizar-mercados/india/llegar-al-consumidor
[68] Kamaishi (Iwate , Japan) - Population Statistics, Charts, Map, Location, Weather and Web Information. (accessed Sep. 03, 2020). https://www.citypopulation.de/php/japan-iwate.php?cityid=03211
[69] Statistical Handbook of Japan 2018, p. 210.
[70] UNdata | record view | City population by sex, city and city type. (accessed Sep. 03, 2020). http://data.un.org/Data.aspx?d=POP&f=tableCode%3a240
[71] The average Dane. (accessed Sep. 03, 2020). https://www.dst.dk/en/Statistik/Publikationer/gennemsnitsdanskeren
[72] High Efficiency 500w 48v Solar Panel Monocrystalline - Buy 500w Panel Solar,500w 48v Solar Panel Monocrystalline, Solar Module 500w Product on Alibaba.com. (accessed Sep. 04, 2020). https://www.alibaba.com/product-detail/high-efficiency-500w-48v-solar-panel_62358163746.html?spm=a2700.7724838.2017115.173.1d2b17bfcp857o&s=p
[73] Bonus-120 zu verkaufen on wind-turbine.com. (accessed Sep. 04, 2020). https://en.wind-turbine.com/wind-turbines/84366/bonus-120-zu-verkaufen.html?utm_source=wind-turbine-models&utm_medium=cpc&utm_campaign=offers
[74] S. S. T. AG, SUNNY TRIPOWER 60 Japan. (accessed Sep. 04, 2020). https://www.sma.de/en/products/solarinverters/sunny-tripower-60-japan.html

Authors' information

[1]Engineering Department, Universidad de Bogotá Jorge Tadeo Lozano, Bogotá 110311, Colombia.

[2]Universidad del Rosario, Faculty of Natural Sciences, Department of Biology, Bogotá 110311, Colombia.

María Fernanda Boada Medina is Environmental Engineer at University of Bogotá Jorge Tadeo Lozano in 2020 and, at present is student in the Specialization of Environmental Law in it. The interests are, among others, design and sizing of PV systems, renewable energy sources, management plans and environmental impact studies, environmental risk management and energy evaluation.

Karen Tatiana Prieto Rojas was a beneficiary of Ser Pilo Paga 2 scholarships delivered by the National Government in 2015. She is a graduate of environmental engineering from the Jorge Tadeo Lozano University in 2020. She obtained the scholarship of excellence for the best average degree in 2019 Interested in topics such as renewable energy, sustainability and conservation. In the future she would like to improve my studies in the area and apply them in the protection and sustainable use of the natural resources of my country.

Fredy Mesa (Corresponding Author): Degree in Physics, Master in 2006 and PhD in Physics (2010) of the National University of Colombia, Bogotá-Colombia. Leader of the NanoTech group of the University of Rosario (full professor) where he has currently carried out research in the field of semiconductors with applications to solar cells, spintronics, biomaterials. Expert in the analysis of electric transport properties in thin films and devices.
E-mail: fredy.mesa@urosario.edu.co

Andres J. Aristizábal is Electrical Engineer and Ph.D in Physics from Universidad Nacional de Colombia. Currently he is the director of the Master in Engineering – Sustainable Energy. His interests are renewable energy, virtual instrumentation, power quality and sustainability. He has published more than forty papers in energy areas.

